International Journal of Environmental Sciences
ISSN: 2229-7359
Vol. 11 No. 7, 2025
https://www.theaspd.com/ijes.php

Enhanced Antibacterial Properties Of Face Mask Decorated With Nitrogen-Doped Carbon Dots And Silver (Ncds/Agnps) Nanocomposites

Luthfiyah Nurul Silmi [1], Surachate Kalasin [*1], Timpika Hormsombut [1], Pantawan Sangnuang [2], Werasak Surareungchai [2]
[1] Faculty of Science, Nanoscience & Nanotechnology Graduate Program, King Mongkut's University of Technology Thonburi (KMUTT), 10140, Bangkok, Thailand
[2] Pilot Plant Research and Development Laboratory, King Mongkut's University of Technology Thonburi, 10150 Bangkok, Thailand

Abstract
Face masks have become an essential part to minimize the spread of bacteria. However, bacteria may develop on the surface of face masks and result in several health issues. The incorporation of silver nanoparticles (AgNPs) can improve the antibacterial properties of face masks. Due to the lack of easily aggregated AgNPs, surface modification with capping agents such as nitrogen-doped carbon dots (NCDs) could improve their stability, antibacterial activity, and prevent aggregation. This study aimed to investigate the antibacterial effect of face masks decorated with NCDs/AgNPs nanocomposites. Therefore, we synthesize NCDs from pineapple peel to prepare NCDs/AgNPs nanocomposites without using toxic chemicals with various $AgNO_3$ concentrations. Face masks coated with NCDs/AgNPs nanocomposites were fabricated by using the dip-coating method at low temperatures (25°C). The antibacterial activities of treated face masks were tested against model gram-positive (Escherichia coli) and gram-negative bacteria (Bacillus subtilis). All treated face mask samples showed better antibacterial activity compared with untreated face masks from the zone of inhibition, colony counting, and inhibition ratio result. The face mask-NCDs/AgNPs 14 ($AgNO_3$ 14 mM) showed the best antibacterial properties with a 99.7% reduction of both bacteria in the colony counting result. The OD600 study also showed the face mask-NCDs/AgNPs 14 have 98.89% and 99.78% inhibition ratio against Escherichia coli and Bacillus subtilis after 12 h. It also demonstrated the contact-killing ability of NCDs/AgNPs on the surface of the face mask from the zone of inhibition result. A higher concentration of $AgNO_3$ in synthesizing NCDs/AgNPs results in a larger nanocomposite size. However, it can provide more antibacterial properties. Thereby, the synergistic effect of NCDs/AgNPs nanocomposites can greatly improve bacterial growth inhibition properties and show a potential to be used as antibacterial agents on face masks
Keywords: *Nitrogen-doped Carbon Dots (NCDs), Silver Nanoparticles (AgNPs), Antibacterial Face Mask, Nanocomposites*

1. INTRODUCTION

Since the SARS-CoV virus has spread globally, wearing face mask have been strongly recommended by the World Health Organization to prevent the infection from being transmitted to anyone anywhere all around the world [1], [2]. It is recommended to reduce the spread of some respiratory diseases related pathogens. However, the bacteria in human saliva and exhaled breath might be a risk to biosafety [3], particularly with long-term face mask usage or face mask reuse, which can lead to several health issues such as pneumonia [1]. It is undeniable that during sneezing, coughing, breathing, or talking, airborne respiratory germs, pathogens, and other microorganisms can attach and be trapped by the face mask and accumulate on the surface of the face mask [3]. At the same time, moisture retention may decrease the face mask's protective properties and creates good condition for bacteria growth [1]. Additionally, the research of face masks coated with antibacterial agents to improve antimicrobial qualities becomes important. Therefore, efforts were made to reduce the spread of bacteria by developing antibacterial materials that are coated on face masks.

Silver nanoparticles (AgNPs) are one of the noble metal nanoparticles that attract a lot of attention [4]. AgNPs have been used for various applications including, food technology 5, cosmetics [5], pharmacology [6], and especially in antibacterial applications. As an antibacterial agent, AgNPs can kill more than 650

different pathogens, including bacteria, viruses, and fungi [7]. They have some properties such as huge surface area, strong thermal stability, and a fast Ag^+ ion release rate that showed promising candidates for antibacterial agents [4].

One method that attracts a lot of attention is synthesizing AgNPs by using carbon dots (CDs). CDs are known as good stabilizers, capping, and reducing agents for the synthesis of metal ions to nanoparticles including AgNPs. The surface of CDs containing abundant oxygen (hydroxyl, carbonyl, carboxyl, and epoxy) makes these CDs excellent electron donors and acceptors for metal nanomaterials [8].

Recently, several methods have been used for synthesizing CDs such as chemical oxidation [9], thermal decomposition [8], ultrasonic microwave irradiation [10], and hydrothermal methods [11]. However, some of the methods required to use toxic chemicals, longtime preparation, and expensive energy equipment. The hydrothermal methods could be an effective method to synthesize CDs due to their easy method and avoidance of using strongly toxic chemicals [12]. Several sources of carbon have been used to synthesize CDs such as sucrose [13], dopamine [14], L-arginine [15], and polyvinylpyrrolidone [16]. However, the use of abundant, low-price, and non-toxic sources of carbon such as biowaste should be used as a precursor of CDs. Subsequently, some of the natural biomasses have been used as a precursor to synthesize CDs, such as corn stalk shells [17], coconut, orange waste peels, and pineapple peel [18], [19], [20]. Pineapple peel has a high carbohydrate content which can be an important carbon source to synthesize CDs [18]. Pineapple peel extract was tested against several microbes and showed antimicrobial activity against B. subtilis, S. aureus, and B. megaterium. Due to the abundant material and potential carbon source, pineapple peel was chosen as a precursor for CDs synthesis in this study.

Furthermore, the chemical and biological activities of CDs can be increased by doping with sulfur (S), boron (B), nitrogen (N), and phosphate (P) during the preparation of CDs [21]. On the other hand, biological activity, antibacterial activity [22], [23], catalytic activity [24], [25]surface reactivity, and chemical activity can be enhanced by N-doping. N-doping is the new class of CDs that can be used to synthesize AgNPs. N-doped CDs (NCDs) act as a stabilized to control the size and morphology of nanocomposites [24]. Therefore, NCDs were used to synthesize NCDs/AgNPs as stabilizing, capping, and reducing agents for improving antibacterial properties. Although there has been significant research on CDs, AgNPs, and antibacterial materials, the specific combination of NCDs/AgNPs from biowaste for antibacterial face mask applications does not exist. CDs are known as good stabilizer, capping, and reducing agents that can be used to reduce metal ions to form nanoparticles including AgNPs. The surface of CDs containing abundant oxygen (hydroxyl, carbonyl, carboxyl, and epoxy) makes these CDs excellent electron donors and acceptors for metal nanomaterials [26]. The chemical and biological activities of CDs can be increased by doping with sulfur (S), boron (B), nitrogen (N), and phosphate (P) during the preparation of CDs29. On the other hand, biological activity, antibacterial activity, catalytic activity, surface reactivity, and chemical activity can be enhanced by nitrogen doping on CDs [27], [28], [29].

Several materials have been successfully used to improve antibacterial activity on face masks by using starch-AgNPs, ZIF-8, AgNPs, and AgNO3-TiO2 [30], [31], [32]. Here in, we used NCDs from pineapple peel to synthesize NCDs/AgNPs nanocomposites by using the reduction method, which methods are a cost-effective, easy, and direct method for synthesizing nanocomposites/nanohybrids using suitable reducing agents [33]. For improving the antibacterial properties of the face mask, the face masks were coated with NCDs/AgNPs nanocomposites and were prepared by using the dip-coating method, this procedure is easy, simple, and the common method used to attach nanocomposites on face masks 38. The face mask nanocomposites were investigated using Escherichia coli as gram-negative bacteria and Bacillus subtilis as gram-positive bacteria by several tests such as clear zone test, colony counting methods, OD 600, and minimum inhibitory concentration to evaluate the antibacterial properties and understand the antibacterial mechanism of the novel face mask NCDs/AgNPs nanocomposites. We believe that face mask nanocomposites have good antibacterial properties, which are important to kill bacteria on the face mask, to prevent infection and transmission of respiratory infectious disease. This research will be promising for the new application in the face mask coated with NCDs/AgNPs as an antibacterial agent and for improving the antibacterial properties of the face mask.

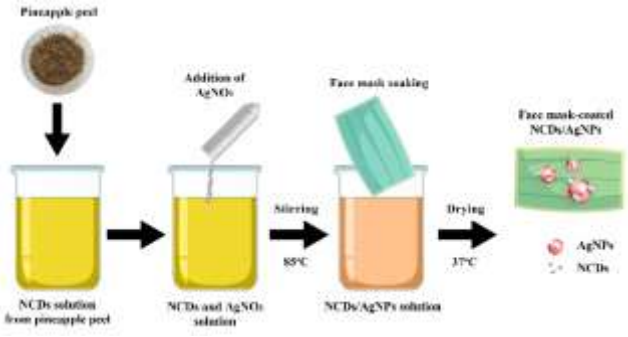

Scheme. 1 Schematic of face mask-NCDs/AgNPs nanocomposite

2. METHOD

2.1 Materials and reagents

Silver nitrate ($AgNO_3$) was purchased from Quality Reagent Chemical Co., Ltd. (QReC™) New Zealand; C_2H_5OH (ethanol) and NH_3 (Ammonia) were bought from Merck KGaA, Darmstadt, Germany; phosphate-buffered saline (1× PBS, 1.8 mM $Na_2HPO_4{\cdot}7H_2O$, 10 mM KH_2PO_4, 137 mM NaCl, and 2.7 mM KCl, pH 7.4) was use d as a control negative in antibacterial study; natrium agar and natrium broth were purchased from HiMedia Laboratories Pvt.Ltd; *Escherichia coli* O157:H7 (DMST 4212) and *Bacillus subtilis* (TISTR 1984) were obtained from the Department of Medical Sciences Thailand and American Type Culture Collection (Manassas, VA); pineapple was purcashed from local market in Thailand; Deionized water with a resistivity of 18.2 MΩ cm was used to prepare the solutions in all the experiment steps; Disposable surgical mask (Siam save, Gennikiz.co.ltd) made from polypropylene (PP) with outer layer: PP spun bond non-woven 20 gsm/2, middle layer: melt blown non-woven 25 gsm/2, inner layer: PP spun bond non-woven 30 gsm/2 were purchased from the local pharmacy market in Thailand.

2.2 Synthesis of nitrogen-doped carbon dots (NCDs)

NCDs were synthesized from pineapple peels as a carbon source using hydrothermal methods. The pineapple peels were washed under running tap water followed by washing using distilled water twice to remove any dust particles. Then the pineapple peels were dried in the oven at 100°C and mashed using a mortar. 2 gr of pineapple peels were dissolved in 25 mL of distilled water with continuous stirring and the ammonia solution was added dropwise until pH 8.5. Next, the solution was transferred into a Teflon-lined autoclave (100 mL) and heated at 200°C for 6 h. After that, the autoclave was cooled down to room temperature. Finally, the dark brown solution was centrifuged at 5000 rpm for 1 hour to separate the precipitate and supernatant solutions, and then the solution was filtered using a filter 0.2 μm membrane to get a clear NCDs solution.

2.3 Synthesis NCDs/AgNPs nanocomposite

NCDs/AgNPs nanocomposites were synthesized using different concentrations of $AgNO_3$ (8 mM, 10 mM, 12 mM, 14 mM) and named NCDs/AgNPs 8, NCDs/AgNPs 10, NCDs/AgNPs 12, and NCDs/AgNPs 14. $AgNO_3$ was used as a precursor while NCDs as a capping, stabilizing, and reducing agent. 20 mL of $AgNO_3$ and 20 mL of NCDs solution were added to a 100 mL reaction flask. The solution was stirred and heated up to 85°C until the color of the solution changed from yellow pale to brown, the color change confirms the formation of NCDs/AgNPs nanocomposite. Finally, the NCDs/AgNPs nanocomposite was stored in the refrigerator at 4°C for further characterization.

2.4 Fabrication of face mask-NCDs/AgNPs

The commercial face mask with 1 cm of diameter was soaked into the solution of NCDs/AgNPs 8, NCDs/AgNPs 10, NCDs/AgNPs 12, and NCDs/AgNPs 14 for 12 hours at room temperature under rotational tubes and named as face mask-NCDs/AgNPs 8, face mask-NCDs/AgNPs 10, face mask-NCDs/AgNPs 12, and face mask-NCDs/AgNPs 14. Then, all samples were dried for 12 hours at room temperature. Face mask-NCDs were fabricated by soaking the face mask in an NCDs solution with the same parameter.

2.5 Antibacterial activity study of face mask-NCDs/Ag

The antibacterial activity study of face mask samples treated with NCDs/AgNPs nanocomposites solution with different concentrations was studied using zone of inhibition against *Escherichia coli* (DMST 4212) (gram-negative bacteria) and *Bacillus subtilis* (TISTR 1984) (gram-positive bacteria). Both bacteria will be cultured in sterile NB media and then stored at 37°C with shaking and incubated until the bacteria concentration is at approximately 10^8 colony forming units (CFU)/mL. After that, the bacterial suspension will be uniformly spread over the agar plates and then a face mask with different concentrations (8 mM, 10 mM, 12 mM, and 14 mM of $AgNO_3$) was placed on the bacterial-coated solid medium plates. Then the solid medium plates were transferred to the 37°C incubator for 24 h. Finally, the diameters of the zone of inhibition (ZOI) were calculated to investigate the antibacterial activity from each sample.

To study the inhibitory effect of face mask- NCDs/AgNPs 8, 10, 12, and 14, the colony counting method was used. Gram-negative *E.coli* (OD_{600} = 0.542, 8D = 1.0 x 10^7 CFU/mL) and Gram-positive *B.subtilis* (OD_{600} = 0.234, 8D = 1.0 x 10^7 CFU/mL) were selected as representative microorganisms and cultured in a medium in the incubator. To examine the inhibitory effect of face mask-NCDs/AgNPs were cut into 1 cm^2 diameter, then the face masks were incubated in 10 mL of bacterial solution which had been diluted 8 times for 24 hours at 37°C in dark condition. 100 µL of the solution was finally spread in solid media and the number of colonies was observed after 12 hours.

$$Bacteria\ Inhibition\ = 1 - \frac{Bacteria\ sample\ colony}{Bacteria\ control\ colony}\ \text{x}\ 100\%$$ [34]

Optical density at 600 nm (OD600) of face mask-NCDs/AgNPs was measured to determine the inhibition ratio against gram-negative (*E.coli*) and gram-positive (*B.subtilis*) bacteria. The bacteria were adjusted to 10^6 CFU/mL using NB media. 1 mL from the bacteria culture was placed on the 1 cm^2 diameter of facemask-NCDs/AgNPs 8, 10, 12, and 14, then incubated at 37°C for 24 hours. To evaluate the inhibition of the bacteria, 200 µL of the cultured bacterial suspension was transferred into a clear bottom 96-well plate and carried out 3 replicate each time. OD600 values were measured every 2 h for 24 h with continuous shaking. The inhibition ratio (%) for bacteria is calculated by:

$$\%\ Inhibition\ ratio = \frac{OD_{untreated} - OD_{sample}}{OD_{control}}\ \text{x}\ 100$$ [35]

2.6 Minimum inhibitory concentration (MIC) of NCDs/AgNPs

To know the minimum inhibitory concentration (MIC) of NCDs/AgNPs as an antibacterial agent, *Escherichia coli* (DMST 4212) (gram-negative bacteria) and *Bacillus subtilis* (TISTR 1984) (Gram-positive bacteria) were used. The bacteria were adjusted to 10^5 using NB broth media and 100 µL bacteria suspension was treated with 100 µL solution of PBS and 100 µL solution NCDs/AgNPs (20 µg/mL, 30 µg/mL, 50 µg/mL, and 60 µg/mL). The suspensions were incubated in 5 mL NB broth medium at 37°C, 120 rpm for 24 h. After that 50 µL of mixed suspension was placed on NA – agar plate and incubated for 24 h. After incubation, the number of colonies was observed.

2.7 Characterization

The absorption and photoluminescence intensity behavior of NCDs, NCDs/AgNPs, and face mask NCDs/AgNPs were carried out with UV-Visible spectroscopy from Cytation 5 with Gen5 3.05 software, (BioTek® Instruments GmbH, Germany) using manual mode (the solution preparation in 96 well plates and the used wavelength around 300-700 nm). The inhibition ratio of OD 600 was performed by using Cytation 5 (manual mode with the solution preparation in 96 well plates and wavelength 600 nm). The hydrodynamic size and zeta potential of NCDs and NCDs/AgNPs in water solvent (25°C) were carried out using dynamic light scattering (DLS) from Malvern Zetasizer, UK. The solution sample (NCDs and NCDs/AgNPs) and solid sample (uncoated and coated face mask) were analyzed under Fourier transform infrared spectroscopy (FTIR), INVENIO R, Bruker, USA. The attenuated total reflectance (ATR) measurement technique (diamond crystal, single bounce) was used to analyze functional groups of samples. Scanning electron microscopy (SEM) and Energy Dispersive Spectroscopy (EDS) of the face mask were carried out using Phenom Pharos (Thermo Scientific, USA) with 5 kV. The NCDs, NCDs/AgNPs,

face mask-NCDs/AgNPs, and face mask-NCDs/AgNPs after the antibacterial test were observed by FESEM (FEI Nova Nanosem U.S). Elemental analysis was investigated by using Energy dispersive X-ray spectroscopy (EDS) (Bruker Nano Xflash 6/3, USA) under 10 kV. The solution sample was deposited on a silicon substrate. Transmission Electron Microscopy (TEM) of NCDs was carried out using the TEM JEM-2100 model (JEOL, USA) with 120 kV accelerating voltage.

3. RESULT AND DISCUSSION

3.1 Characterization result of NCDs

NCDs solution was synthesized from pineapple peel using the hydrothermal method and showed pale yellow color under normal light and blue fluorescence color under UV light (Fig. 1a inset). The fluorescence emission spectrum was used to check the excitation-emission properties. As shown in Fig.1a. NCDs were excited at different excitation wavelengths and showed the excitation-dependent emission property of NCDs with the maximum emission peak at 380 nm occurring at the excitation wavelength of 310 nm.

To characterize the optical properties and the information about the absorption behavior of NCDs we use UV-Visible spectroscopy analysis. The UV–Visible absorption spectra of the NCDs band were recorded in the range of 300–700 nm. Fig.1b shows the results from UV-Vis spectroscopy that the fabricated NCDs have a maximum surface plasmon resonance (SPR) λ_{max} at 320 nm which was attributed to the typical absorption of NCDs associated with the π–π^* transition band C=O –π^* transition band C=C. Similar results were shown in other work which confirms the successful synthesis of NCDs [36], [37], [38].

FTIR was used to analyze functional groups of NCDs (Fig.1c) NCDs sample showed two broad peaks at 3634 cm^{-1} and 3325 cm^{-1} indicating the presence of O-H peaks, the present two O-H peaks in the O-H group means the hydrogen bonding occurs when the O-H group interact with the electronegative atom, such as nitrogen in this sample. O-H in peak 3325 cm^{-1} corresponds to the hydroxyl group and the presence of strong hydrogen bonds, while O-H in peak 3634 cm^{-1} corresponds to the hydroxyl groups with weaker hydrogen bonds or those with little to no hydrogen bonding. While bands at 1815 cm^{-1} were present due to C-H bending. Bands at 1645 cm^{-1}, 1485 cm^{-1}, and 1335 cm^{-1} from NCDs were observed due to C=N stretching, C-H bending, and C-N stretching. These results suggest that NCDs have aromatic structures with abundant amino and phenol hydroxyl groups on the surface and act as electron donors for the reduction of Ag^+.

a

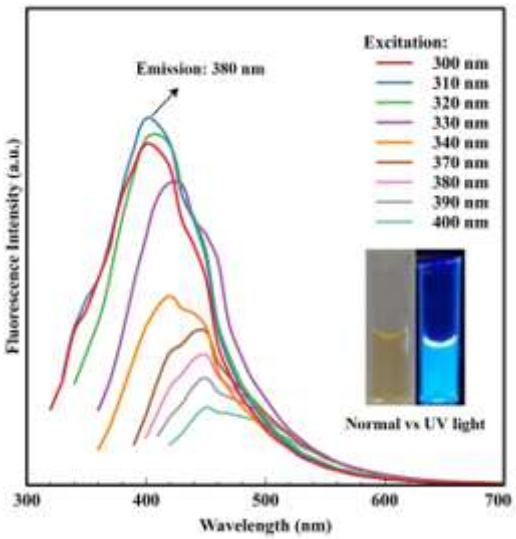

b

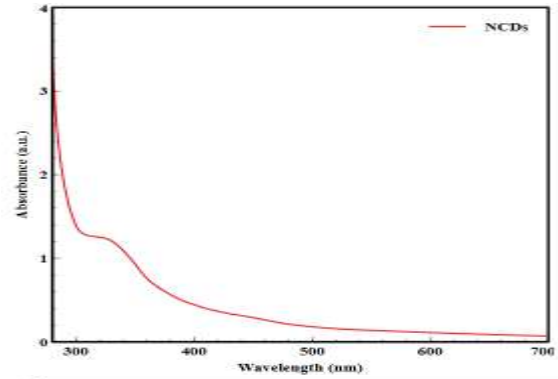

c

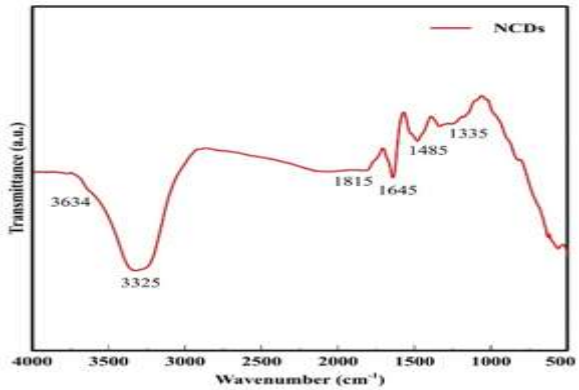

Fig. 1 Characterization result of NCDs. **(a)** Fluorescence intensity; **(b)** UV-Visible spectroscopy; **(c)** FTIR result.

Transmission electron microscopy (TEM) was used to determine the morphology, size, and structure of the NCDs. The NCDs are uniformly spherical morphology dispersed (Fig.2a) and show a mean distribution size ranging from 2 nm to 5 nm and can be observed with the average particle size is 3.189 nm (Fig.2b). From this result, there is no significant aggregation and the NCDs are well dispersed, it can be indicated that the NCDs also have high stability. Moreover, NCDs also have the distribution of C, N, and O elements that was observed from the EDS result (Fig.S1), and the Si element was detected due to the use of a silicon wafer. These findings show that pineapple peel was effectively used as an NCDs source and has a promising application for synthesizing NCDs/AgNPs.

a

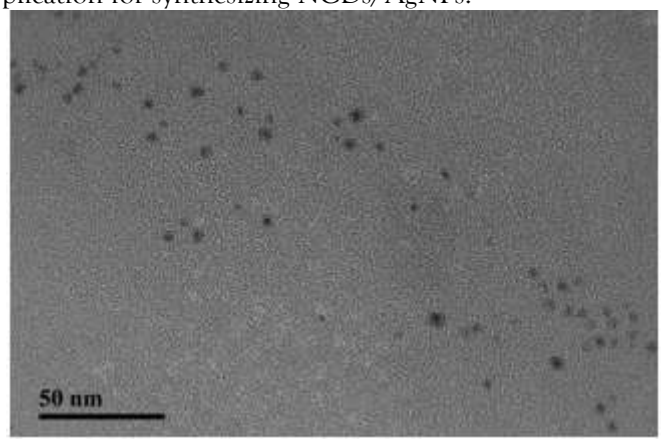

b

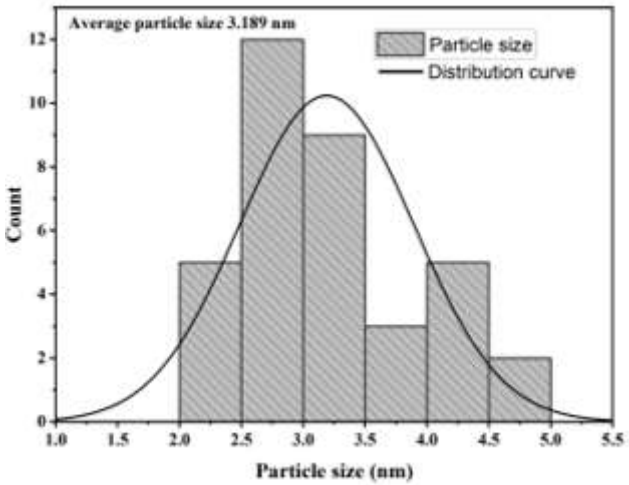

Fig. 2 TEM result of NCDs

3.2 Characterization result of NCDs/AgNPs

The formation of NCDs/AgNPs from all samples was indicated by a color change from yellow to brown that appeared in all samples at 90 min (Fig.S2). The fluorescence intensity result of NCDs/AgNPs in different concentrations of $AgNO_3$ as precursor shows that more concentration of $AgNO_3$ can cause a lower fluorescence emission peak of NCDs/AgNPs nanocomposite below the excitation wavelength of NCDs at 310 nm, which may be due to silver ions inducing electron transfer between NCDs and AgNPs[39] (Fig.3a). In the UV-Visible spectroscopy results of NCDs/AgNPs nanocomposite, all samples exhibited a new absorption peak at 430 nm for NCDs/AgNPs 8 and NCDs/AgNPs 10 and 470 nm for NCDs/AgNPs 12 and NCDs/AgNPs 14 (Fig.3b). This result indicates that all samples showed the specific absorption peak of AgNPs [40] An increase in reaction time results in an increase in the absorbance peak around the wavelength of 430-470 nm and produce the formation of NCDs/AgNPs nanocomposite in 90 minutes (Fig.S2). Therefore, the 90 min reaction time was used for all the NCDs/AgNPs nanocomposite synthesis. The similar absorbance peaks were observed after 3 months at 4°C stored and showed no aggregation or degradation was observed within 3 months of storage from all samples. From the result, we can indicate the effect of NCDs acting as reducing and stabilizing agents for NCDs/AgNPs (Fig.S3).

a

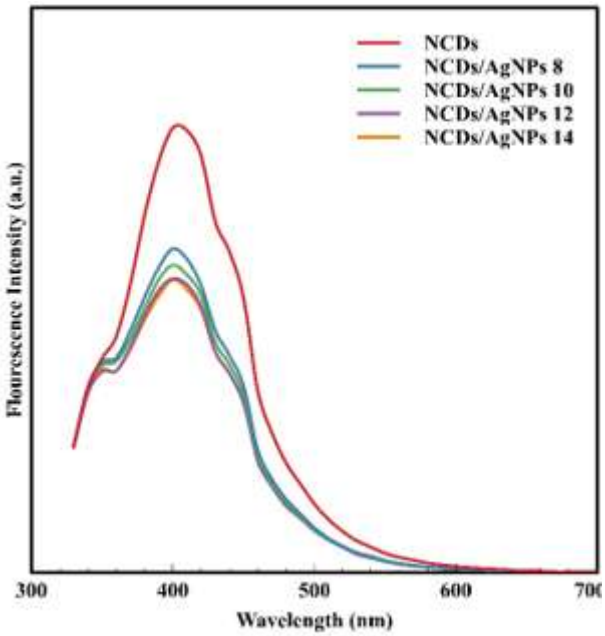

b

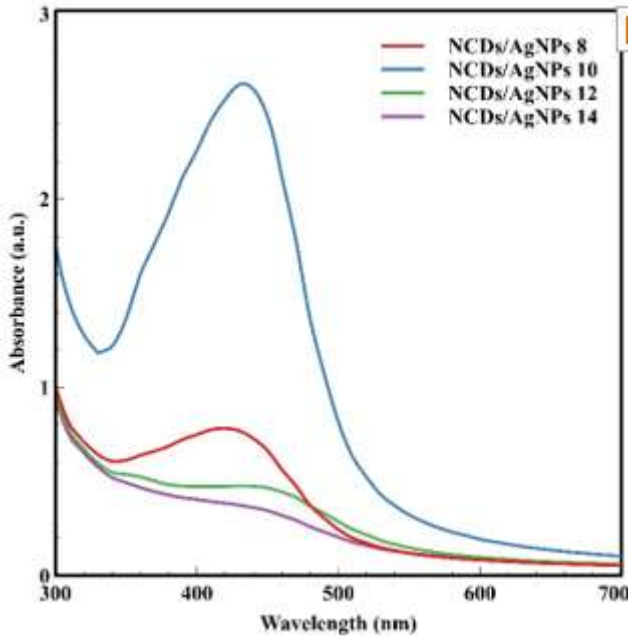

Fig. 3 Optical properties of NCDs/AgNPs. **(a)** Fluorescence intensity; **(b)** UV-Vis spectroscopy

The dynamic light scattering (DLS) technique was used to determine the hydrodynamic size distribution of NCDs/AgNPs. As shown in Fig.4a, the hydrodynamic size at 47.8 nm, 43.8 nm, 50.7 nm, and 68.1 nm was observed from NCDs/AgNPs 8, NCDs/AgNPs 10, NCDs/AgNPs 12, and NCDs/AgNPs 14 sample. NCDs/AgNPs 14 showed the biggest size while NCDs/AgNPs 10 showed the smallest size. This result is in good agreement with the UV-Vis absorption result that the wide peak may lead to larger particle sizes [41]. Zeta potential was used to study the stability and surface charge of samples. As shown in Fig.4b, NCDs showed a negative zeta potential (-15 mV) and have a similar result from other research [42], [43], [44] This high negative value can produce a repulsive force to stabilize the synthesized NCDs/AgNPs nanocomposites [45]. Moreover, the increased concentration of $AgNO_3$ in the synthesis of NCDs/AgNPs caused the higher negative value of zeta potential, -22.4 mV for NCDs/AgNPs 8, -27.7 mV for NCDs/AgNPs 10, -32.1 mV for NCDs/AgNPs 12, and -33.4 mV for NCDs/AgNPs 14 which indicate good stability of the synthesized NCDs/AgNPs [46]. The negative charge of NCDs/AgNPs can lead to the potential interaction with the bacterial membrane, the electrodynamic repulsive forces are weaker than the shear force, causing them to interact [47]. The zeta potential of NCDs/AgNPs after 3 months of storage also showed a similar value with fresh NCDs/AgNPs which indicated NCDs as stabilizing agents (Fig.S4).

FTIR was used to analyze functional groups of NCDs/AgNPs. Fig.4c shows spectra of NCDs/AgNPs nanocomposite in different concentrations of $AgNO_3$, several peaks from NCDs also appeared but shifted from 1485 cm^{-1} to 1567 cm^{-1} (C-H bending) and 1335 cm^{-1} to 1369 cm^{-1} (C-N stretching) due to the reaction between NCDs and AgNPs to form NCDs/AgNPs nanocomposite. C, N, O, and Ag elements also appeared in NCDs/AgNPs samples from FESEM-EDS results (Fig.S5-S8). These results can confirm the successful synthesis of NCDs/AgNPs with NCDs as reducing agents for antibacterial face masks.

a

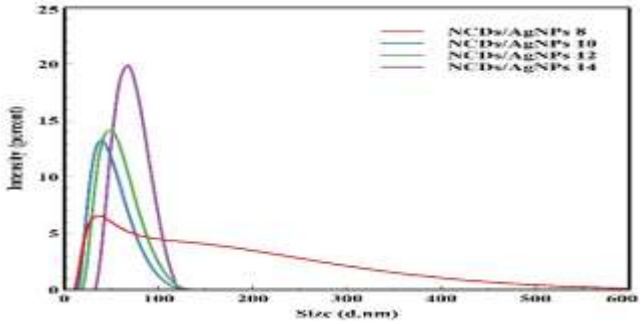

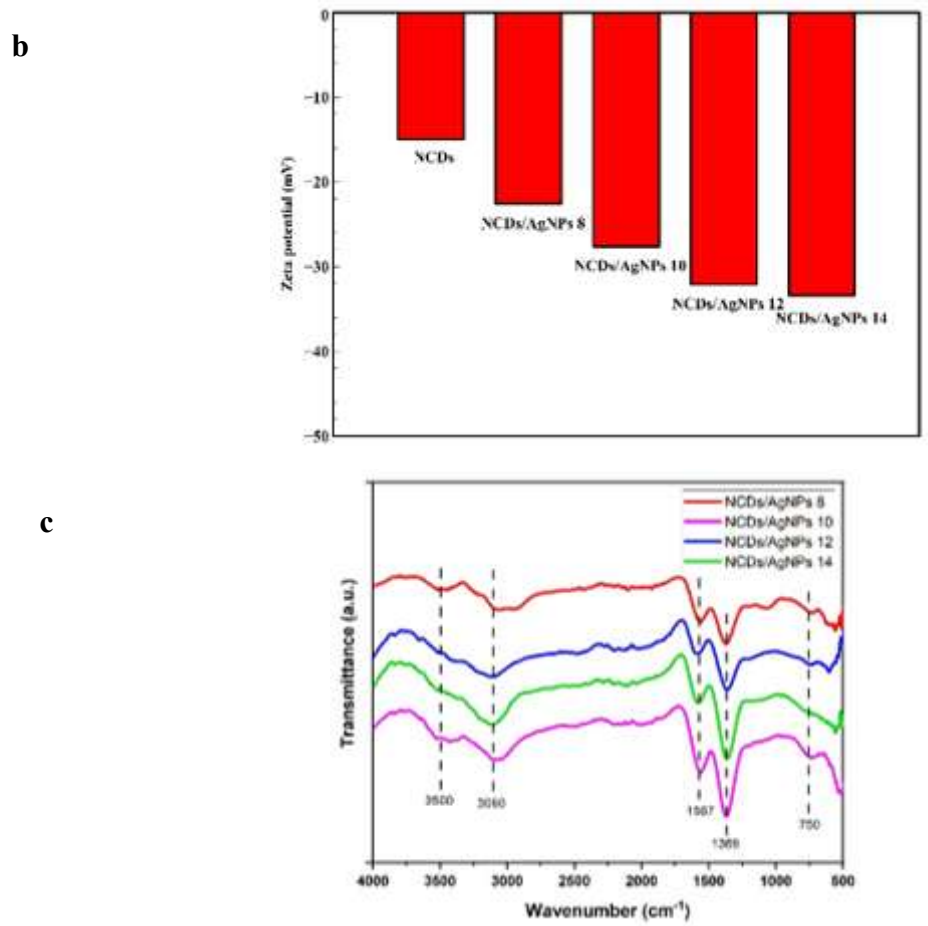

Fig. 4 Characterization result of NCDs/AgNPs. **(a)** Hydrodynamic size; **(b)** Zeta potential; **(c)** FTIR result.

3.3 Characterization result of face mask-NCDs/AgNPs

The comparison of untreated and treated face masks with NCDs/AgNPs nanocomposite was further confirmed by the FTIR measurement (Fig.5a). The new bands at 3635 cm^{-1} (O-H stretching), 1485 cm^{-1} (C-H bending), and 1345 cm^{-1}(C-N stretching) were present due to the presence of NCDs/AgNPs nanocomposite on the surface of the face mask. Moreover, the higher concentration of $AgNO_3$ in the formation of NCDs/AgNPs nanocomposite caused more stretching in those peaks and indicated more NCDs/AgNPs nanocomposite on the surface of the face mask.

The surface morphology of untreated and treated face masks was examined by FESEM-EDS analysis carried out to identify the morphology and element's presence on the face mask NCDs and NCDs/AgNPs. A significant difference was seen between the untreated face masks which had a smooth surface (Fig.S9) and the EDS result showed the elemental analysis that presents only carbon (C) element (Fig.S9), whereas the face masks treated with NCDs/AgNPs nanocomposite had a slightly rough surface (Fig.5b, Fig.S10), which could be attributed to the deposition of NCDs/AgNPs nanocomposite onto the surface of the face mask. All of the face mask-NCDs/AgNPs EDS results showed C, N, O, and Ag elements (Fig.5c, Fig.S11). Moreover, all the elemental mapping results of face mask-NCDs/AgNPs showed the distribution of C, N, O, and Ag from the NCDs/AgNPs on the surface of face mask. These results indicated the successful fabrication of treated face masks with NCDs/AgNPs as antibacterial agents (Fig.5d).

a

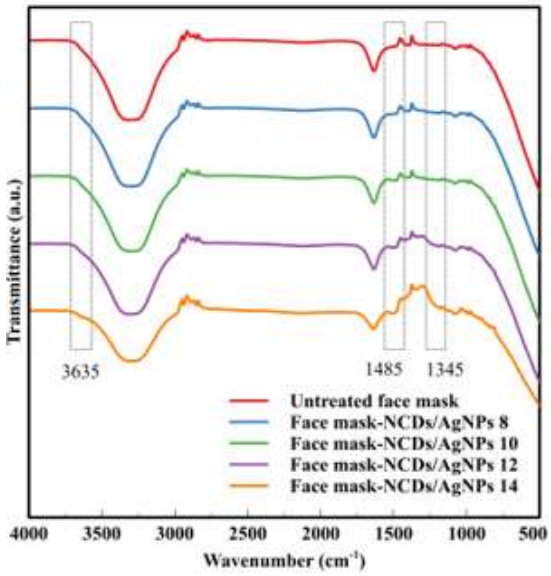

b

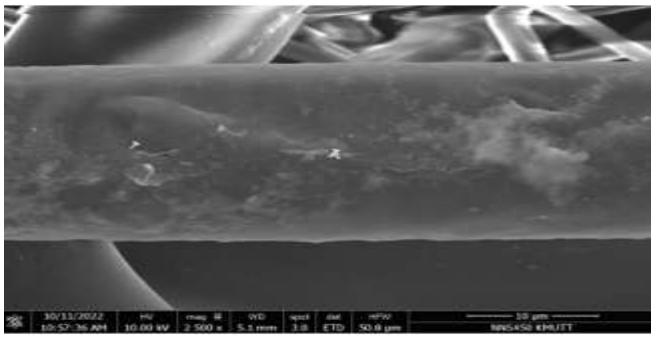

c

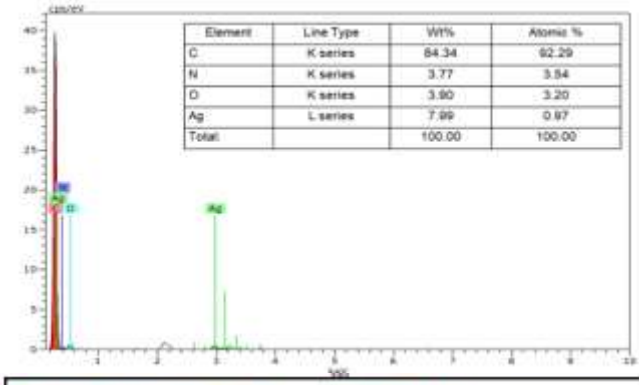

Element	Line Type	Wt%	Atomic %
C	K series	84.34	92.29
N	K series	3.77	3.54
O	K series	3.90	3.20
Ag	L series	7.99	0.97
Total:		100.00	100.00

d

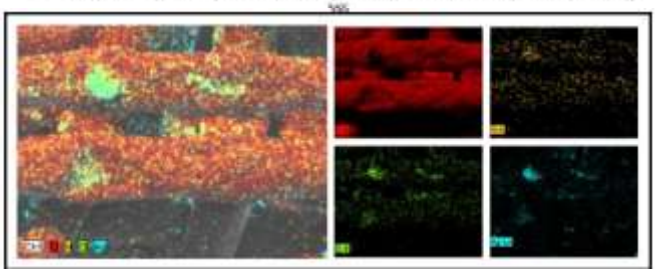

Fig. 5 (a) FTIR result of untreated and treated face mask; **(b)** FESEM, **(c)** EDS, and **(d)** EDS mapping result of NCDs/AgNPs 14

3.4 Antibacterial activity result

The antibacterial activity of the treated face mask was investigated by the zone of inhibition, colony counting methods, and inhibition ratio using spectrophotometer methods by measuring optical density

(OD600). In every test antibacterial activity of untreated face masks, face mask-NCDs, and face mask-NCDs/AgNPs were tested against gram-negative bacteria (*E. coli*) and gram-positive bacteria (*B. subtilis*). The zone of inhibition result of untreated and treated face masks is shown in Fig.6, the untreated face mask and face mask-NCDs sample did not appear inhibition zone for *E. coli* and *B. subtilis* bacteria which means the untreated face mask and face mask-NCDs had no antibacterial effect. However, all face mask-NCDs/AgNPs nanocomposite samples showed antibacterial activity against both gram-positive and gram-negative bacteria. As shown in Table 1, face mask NCDs/AgNPs 14 have the highest zone of inhibition, with a diameter clear zone is 11.33 mm against *E.coli* and 13.33 mm for *B. subtilis*. All samples of face mask-NCDs/AgNPs nanocomposite showed less antibacterial activity against gram-negative bacteria (*E. coli*) than gram-positive bacteria (*B. subtilis*) due to the phosphor phospholipids of the outer membrane of gram-negative bacteria react with metal cations [48], reducing the metal cations that pass through the cell wall and weakening the anti-bacterial reaction, and also cell wall of Gram-negative bacteria is a multilayer structure, which contains a thin peptidoglycan layer, a lipoprotein layer, phospholipids, or a lipopolysaccharide layer. This complex layer structure attenuates the interaction between NCDs/AgNPs nanocomposite and cells. While the cell wall of gram-positive bacteria is composed of a thick but single layer of peptidoglycan. On the other hand, Gram-positive bacteria consist of a single layer of peptidoglycan and lack an outer membrane to react with metal cations. Thus, a higher concentration of metal cations can attack Gram-positive bacteria, causing a higher antibacterial effect so that it is easy to interact with NCDs/AgNPs nanocomposite[49]. A larger diameter of the inhibition zone was found in line with increasing $AgNO_3$ concentration in NCD/AgNPs synthesis that was applied on the face mask. The highest zone of inhibition was observed in the face mask-NCDs/AgNPs 14 sample which can release more Ag^+ ions to inactivate bacteria[50].

a

b

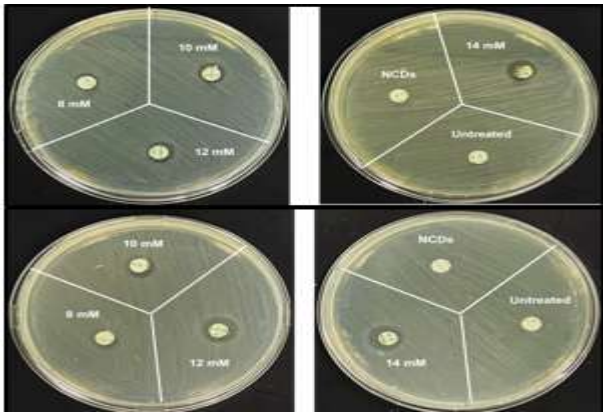

Fig 6. The inhibition zone of untreated face mask, face mask-NCDs, face mask-NCDs/AgNPs 8, face mask-NCDs/AgNPs 10, face mask-NCDs/AgNPs 12, and face mask-NCDs/AgNPs 14 against **(a)** *E. coli* bacteria **(b)** *B. subtilis* bacteria

Table 1 The inhibition zone result

Sample	***Diameter of the clear zone (mm)***	
	E. coli	***B. subtilis***
Untreated face mask	*0*	*0*
Face mask-NCDs	*0*	*0*
Face mask-NCDs/AgNPs 8	*7.33 ± 0.88*	*9.33 ± 0.88*
Face mask-NCDs/AgNPs 10	*9.00 ± 0.57*	*11.00 ± 0*
Face mask-NCDs/AgNPs 12	*10.67 ± 0.33*	*11.67 ± 0.88*
Face mask-NCDs/AgNPs 14	*11.33 ± 0.33*	*13.33 ± 0.33*

FESEM imaging provides high-resolution images that allow for detailed visualization of the face mask sample surface. In the context of antibacterial tests, if no bacteria are observed in the images, it indicates that the nanocomposites have created a zone of inhibition around the sample area, where the bacterial growth has been inhibited or eradicated. The FESEM images result of face mask-NCDs/AgNPs 14 against *E. coli* and *B. subtilis* were shown in Fig.7**.** This result showed no sign of bacteria which can be indicated that face mask-NCDs/AgNPs 14 have successfully inhibited or killed the bacteria present in the test area. Furthermore, it also demonstrated the contact-killing ability of NCDs/AgNPs on the surface of the face mask. This result can lead to the potential of NCDs/AgNPs nanocomposite for improving the antibacterial activity of face masks.

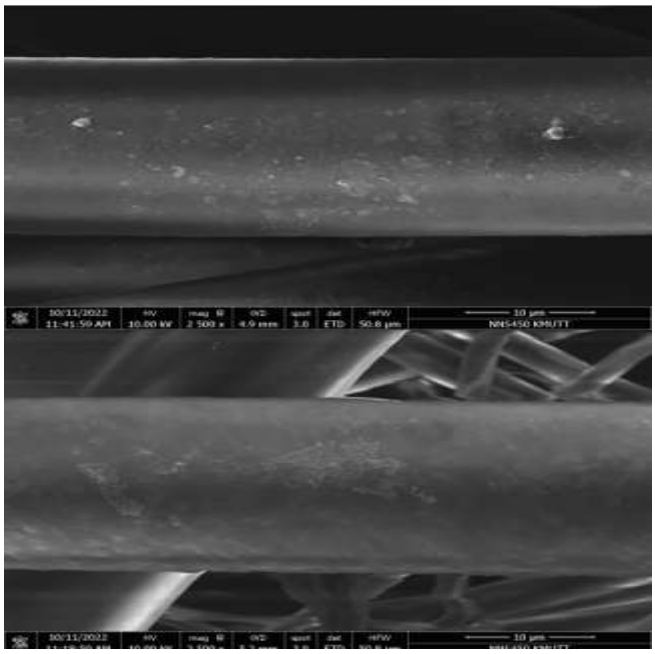

Fig. 7 FESEM images of Face mask-NCDs/AgNPs 14 after zone of inhibition test against **(a)** *E. coli* and **(b)** *B. subtilis*

The viable CFU reduction because of antimicrobial activity can be calculated by comparing the colony counts from samples with and without samples. A reduced number of CFUs on an agar plate indicates that the samples have an antibacterial effect. The antibacterial activity of face mask-NCDs/AgNPs 8, 10, 12, and 14 were also evaluated using colony counting methods. As shown in Fig.8, the lower CFU was observed when the concentration of $AgNO_3$ increased in NCDs/AgNPs synthesis. When the face mask-NCDs/AgNPs 12 the inhibitory effect on *E.*coli was 95%, while the inhibitory effect of *B.subtilis* was 98.3%. At the face mask-NCDs/AgNPs 14 showed no CFU which indicated the best reduction of bacteria with 99.7% inhibitory effect on *E.coli* and *B.subtilis*.

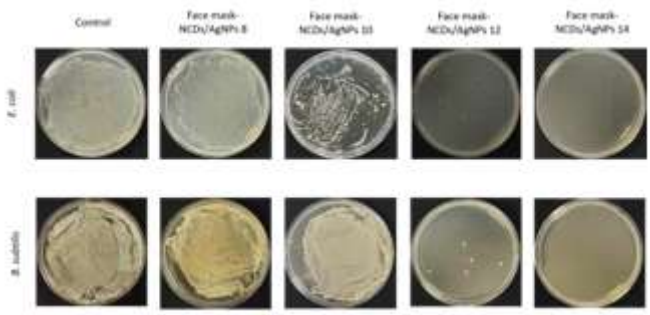

Fig 8. Colony counting methods of face mask NCDs/AgNPs 8, 10, 12, and 14 results.

The inhibition effect of face mask-NCDs/AgNPs against *E.coli* and *B.subtilis* were measured using OD 600 methods. As shown in Fig.9, compared to untreated face masks, all of the treated face masks has a

lower value of OD 600 and was close to zero for face mask 14 and face mask 12 when the contact time was more than 20 h against *E.coli*, indicating the affinity between the bacterial cell and the face mask. The treated face masks also showed a better ability to inhibit the growth of *B. subtilis* compared to the uncoated face mask. Face masks-NCDs/AgNPs 14 can inhibit bacterial growth of *B. subtilis* for up to 16 h and start inhibiting bacteria again at 20 h.

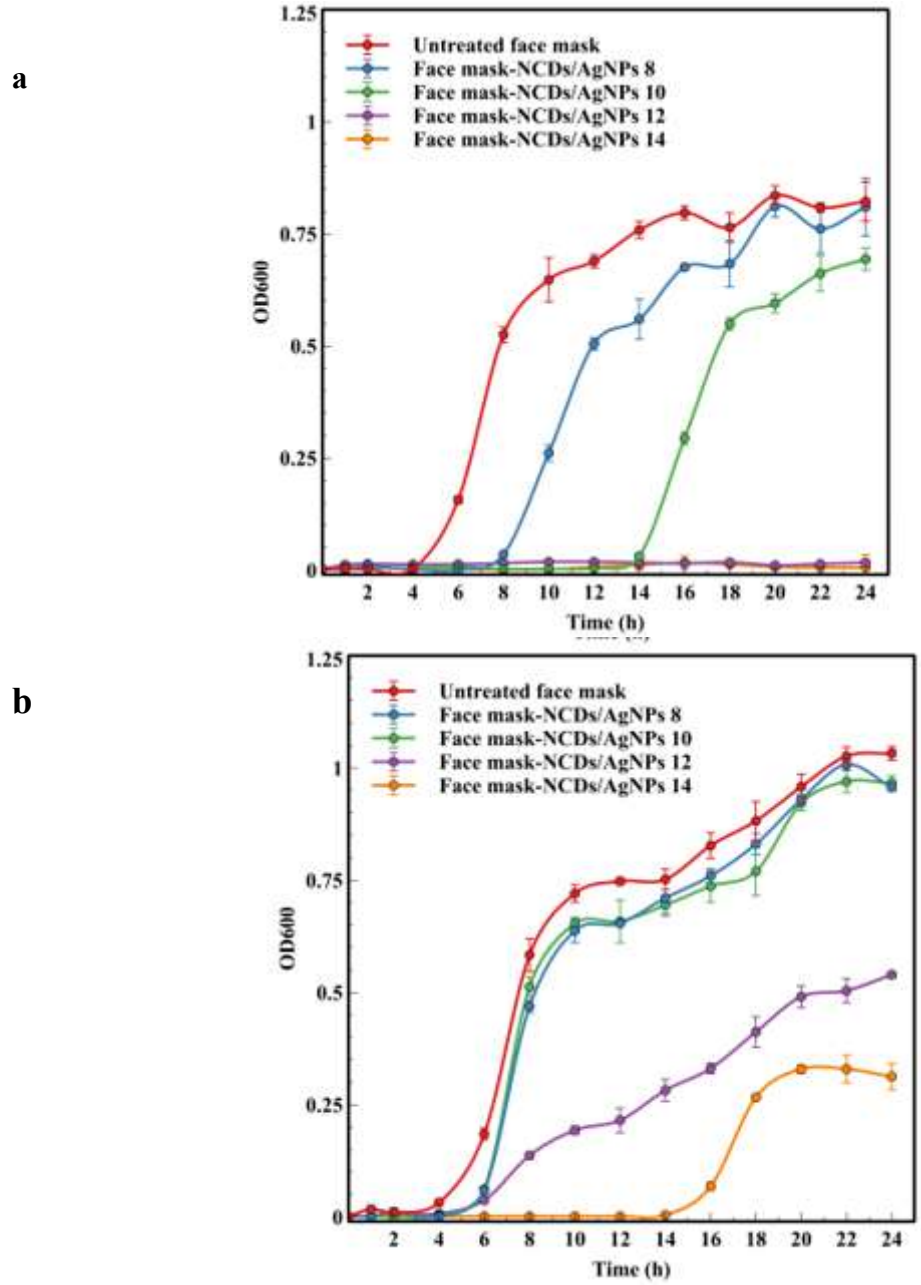

Fig 9. OD 600 result of untreated and treated face mask. **(a)** *E. coli* bacteria; **(b)** *B. subtilis*

The inhibition ratio of face mask-NCDs/AgNPs against *E.coli* and *B.subtilis* shown in Table 2. As we expected, face mask NCDs/AgNPs 14 showed effective antibacterial activities against both bacteria. The inhibition ratio of face mask-NCDs/AgNPs 14 against *E.coli* and *B.subtilis* after 12 h was 98.89% and 99.78% while the inhibition ratio of 99.28% and 69.72% was observed after 24 h against *E.coli* and *B.subtilis*. Face mask-NCDs/AgNPs 12 also has effective antibacterial activities with an inhibition ratio was 97.93% against *E.coli* and 47.74% against *B.subtilis* after 24 h. In contrast with the inhibition ratio of face mask-NCDs/AgNPs 8 and 10 have low effective antibacterial activity against both bacteria after 24 h.

Table 2. The inhibition ratio of face mask-NCDS/AgNPs against *E.coli* and *B.subtilis*

Sample	Inhibition ratio of *B.subtilis* (%)			Inhibition ratio of *E.coli* (%)		
	6 h	12 h	24 h	6 h	12 h	24 h
Face mask-NCDs/AgNPs 8	67.99	12.53	7.36	99.79	26.74	1.50
Face mask-NCDs/AgNPs 10	66.37	11.95	6.42	95.12	99.37	15.65
Face mask-NCDs/AgNPs 12	79.68	71.15	47.74	91.51	97.29	97.93
Face mask-NCDs/AgNPs 14	99.10	99.78	69.72	98.73	98.89	99.28

Face mask-NCDs/AgNPs 14 showed the best results from the agar diffusion test, and colony counting methods, further experiments were carried out to determine the minimum inhibitory concentration (MIC) of NCDs/AgNPs 14 against *E. coli* and *B. subtilis*. Increasing the concentration of NCDs/AgNP 14 resulted in lower colony growth, which means that higher concentrations resulted in more effective antibacterial activity. As shown in Fig.10, low concentrations of NCDs/AgNPs 14 showed excellent bacterial killing efficiency, with the total killing of *E. coli* and *B. subtilis* at 60 µg/mL and 30 µg/mL. AgNPs from NCDs/AgNPs can diffuse freely into the culture medium and can act as a biocidal agent [51]. NCDs/AgNPs showed a better antibacterial effect against *B.subtilis* than *E. coli*. This result is in line with the agar diffusion test from the face mask-NCDs/AgNPs results. Therefore, NCDs/AgNPs nanocomposites exhibit superior antibacterial properties and can be applied as antibacterial agents in face masks.

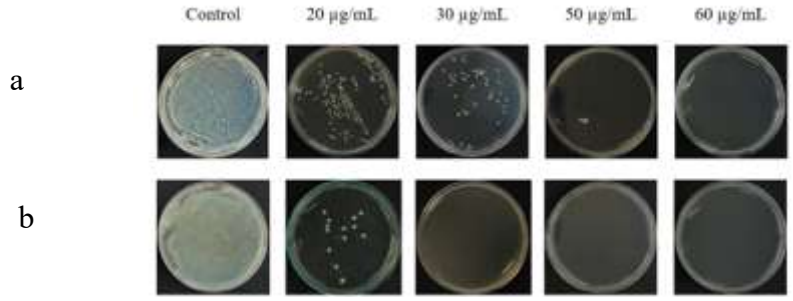

Fig 10. Minimum Inhibitory concentration of NCDs/AgNPs 14 result. **(a)** *E.coli* and **(b)** *B.subtilis*.

It is important to consider both qualitative and quantitative measurements to assess the material's antibacterial effects against different bacterial strains and to evaluate their potential for use in antibacterial face masks. Thus, Comprehensive assessment of NCDs/AgNPs nanocomposites coated on face masks through the zone of inhibition, colony counting method, and OD600 method provides their antibacterial properties evaluation and helps validate the results to be applied as potential antibacterial agents on face masks.

3.5 **Antibacterial activity mechanism**

From the antibacterial studies, we can indicate that NCDs/AgNPs play a significant role in killing bacteria on the face mask. As NCDs act as stabilizing, reducing, and capping agents for AgNPs, these allow NCDs/AgNPs to provide more antibacterial properties on face masks. As airborne bacteria can be captured by a treated face mask with NCDs/AgNPs nanocomposite, the antibacterial agents of NCDs/AgNPs nanocomposites can destroy the cell and generate reactive oxygen species (ROS) to kill bacteria on the surface of the face mask. The bacterial destruction mechanism is illustrated in Fig.11. AgNPs can kill bacteria by inhibiting bacterial growth through interference with the bacterial respiratory

function, or by binding to and destroying the bacterial cell wall [52]. Then, the NCDs/AgNPs kill and prevent bacteria to enter the respiratory system.

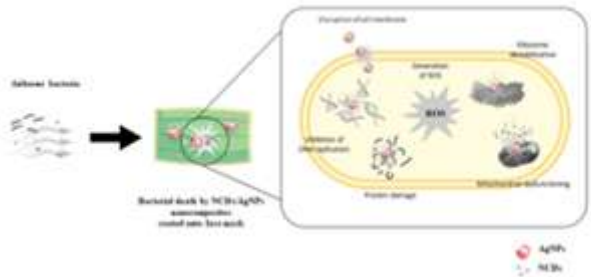

Fig 11. Schematic of the antibacterial mechanism of face mask coated with NCDs/AgNPs nanocomposite

4. CONCLUSION

This study has reported the antibacterial activity of NCDs/AgNPs coated onto face masks as a potential personal protective material to prevent infection and transmission of respiratory infectious disease from human exhaling. The NCDs/AgNPs nanocomposites have been synthesized in one step of fabrication without the use of toxic chemicals. NCDs act as a stabilizing, reducing, and capping agent for NCDs/AgNPs. The antibacterial face masks were prepared by coating commercial face masks with NCDs/AgNPs nanocomposites at room temperature using dip-coating methods. The UV-Vis, PL spectrum, DLS, FTIR, TEM, and FESEM EDS results confirm the successful synthesis of NCDs, NCDs/AgNPs nanocomposites, and the fabrication of antibacterial face masks. And the zeta potential of NCDs/AgNPs nanocomposite indicated that the nanocomposite possesses excellent stability. Furthermore, the antibacterial face masks were tested with gram-positive and gram-negative bacteria. All treated face mask samples showed better antibacterial activity compared with untreated face masks. The higher concentration of $AgNO_3$ in the synthesis of NCDs/AgNPs resulted in a larger nanocomposite size because the NCDs used as stabilizers, reducing agents, and capping agents were used less but can provide more antibacterial properties in face masks. It confirmed that NCDs/AgNPs nanocomposite played an important role in inhibiting the growth of bacteria and acting as promising antibacterial agents on the face mask. Overall, the face mask-NCDs/AgNPs 14 also showed no intact bacteria and demonstrated the contact-killing ability of NCDs/AgNPs on the surface of the face mask. This result can lead to the potential of NCDs/AgNPs nanocomposite for improving the antibacterial activity of face masks.

Author Contributions

L.N.S. wrote the manuscript with guidance from S.K. and W.S.; L.N.S., T.H., and P.S. carried out the experiments. S.K. and W.S. supervised the project, edited, and reviewed the manuscript.

Conflicts of interest

There are no conflicts to declare.

Acknowledgments

We thank KMUTT for providing the Petchra Pra Jom Klao master's degree scholarship to Mrs. Luthfiyah N. Silmi. We also thank the Sensor Technology laboratories at King Mongkut's University of Technology Thonburi for facilitating the use of space and equipment for this research.

REFERENCES

[1] W. W. Nazaroff and C. J. Weschler, "Cleaning products and air fresheners: exposure to primary and secondary air pollutants," *Atmos Environ*, vol. 38, no. 18, pp. 2841–2865, 2004.

[2] C. Wang, P. W. Horby, F. G. Hayden, and G. F. Gao, "A novel coronavirus outbreak of global health concern," *The lancet*, vol. 395, no. 10223, pp. 470–473, 2020.

[3] A. A. Chughtai *et al.*, "Contamination by respiratory viruses on outer surface of medical masks used by hospital healthcare workers," *BMC Infect Dis*, vol. 19, no. 1, p. 491, 2019.

[4] T. C. Mokhena and A. S. Luyt, "Electrospun alginate nanofibres impregnated with silver nanoparticles: Preparation, morphology and antibacterial properties," *Carbohydr Polym*, vol. 165, pp. 304–312, 2017.

[5] Q. Abbas *et al.*, "Green synthesis of silver nanoparticles using Bidens frondosa extract and their tyrosinase activity," *Iran J Pharm Res*, vol. 16, no. 2, p. 763, 2017.

[6] J. Anquetin, S. Deschamps, and J. Claude, "The rediscovery and redescription of the holotype of the Late Jurassic turtle Plesiochelys etalloni," *PeerJ*, vol. 2, p. e258, 2014.
[7] S. Medici, M. Peana, V. M. Nurchi, and M. A. Zoroddu, "Medical uses of silver: history, myths, and scientific evidence," *J Med Chem*, vol. 62, no. 13, pp. 5923–5943, 2019.
[8] J. Wang, C. Wang, and S. Chen, "Amphiphilic egg-derived carbon dots: rapid plasma fabrication, pyrolysis process, and multicolor printing patterns," *Angewandte Chemie-International Edition*, vol. 51, no. 37, p. 9297, 2012.
[9] A. Suryawanshi *et al.*, "Large scale synthesis of graphene quantum dots (GQDs) from waste biomass and their use as an efficient and selective photoluminescence on–off–on probe for Ag+ ions," *Nanoscale*, vol. 6, no. 20, pp. 11664–11670, 2014.
[10] Y.-Y. Yao, G. Gedda, W. M. Girma, C.-L. Yen, Y.-C. Ling, and J.-Y. Chang, "Magnetofluorescent carbon dots derived from crab shell for targeted dual-modality bioimaging and drug delivery," *ACS Appl Mater Interfaces*, vol. 9, no. 16, pp. 13887–13899, 2017.
[11] A. A. Kajani, L. Rafiee, S. H. Javanmard, N. Dana, and S. Jandaghian, "Carbon dot incorporated mesoporous silica nanoparticles for targeted cancer therapy and fluorescence imaging," *RSC Adv*, vol. 13, no. 14, pp. 9491–9500, 2023.
[12] M.-M. Titirici, M. Antonietti, and N. Baccile, "Hydrothermal carbon from biomass: a comparison of the local structure from poly-to monosaccharides and pentoses/hexoses," *Green Chemistry*, vol. 10, no. 11, pp. 1204–1212, 2008.
[13] X. Wei *et al.*, "Facile synthesis of a carbon dots and silver nanoparticles (CDs/AgNPs) composite for antibacterial application," *RSC Adv*, vol. 11, no. 30, pp. 18417–18422, 2021.
[14] J. Jana, S. S. Gauri, M. Ganguly, S. Dey, and T. Pal, "Silver nanoparticle anchored carbon dots for improved sensing, catalytic and intriguing antimicrobial activity," *Dalton Transactions*, vol. 44, no. 47, pp. 20692–20707, 2015.
[15] B. Liu, C. Yao, and S. Fang, "Evaluation of a non-woven fabric coated with a chitosan bi-layer composite for wound dressing," *Macromol Biosci*, vol. 8, no. 5, pp. 432–440, 2008.
[16] Y. Dai, J. Wang, P. Tao, and R. He, "Various hydrophilic carbon dots doped high temperature proton exchange composite membranes based on polyvinylpyrrolidone and polyethersulfone," *J Colloid Interface Sci*, vol. 553, pp. 503–511, 2019.
[17] Z. Li *et al.*, "Green synthesis of carbon quantum dots from corn stalk shell by hydrothermal approach in near-critical water and applications in detecting and bioimaging," *Microchemical Journal*, vol. 166, p. 106250, 2021.
[18] K. Abinaya, S. K. Rajkishore, A. Lakshmanan, R. Anandham, P. Dhananchezhiyan, and M. Praghadeesh, "Synthesis and characterization of carbon dots from coconut shell by optimizing the hydrothermal carbonization process.," *Journal of Applied & Natural Science*, vol. 13, no. 4, 2021.
[19] S. Rajamanikandan, M. Biruntha, and G. Ramalingam, "Blue emissive carbon quantum dots (CQDs) from bio-waste peels and its antioxidant activity," *J Clust Sci*, vol. 33, no. 3, pp. 1045–1053, 2022.
[20] A. Prasannan and T. Imae, "One-pot synthesis of fluorescent carbon dots from orange waste peels," *Ind Eng Chem Res*, vol. 52, no. 44, pp. 15673–15678, 2013.
[21] Z. Zhang *et al.*, "A minireview on doped carbon dots for photocatalytic and electrocatalytic applications," *Nanoscale*, vol. 12, no. 26, pp. 13899–13906, 2020.
[22] W.-J. Niu, R.-H. Zhu, H.-B. Zeng, S. Cosnier, X.-J. Zhang, and D. Shan, "One-pot synthesis of nitrogen-rich carbon dots decorated graphene oxide as metal-free electrocatalyst for oxygen reduction reaction," *Carbon N Y*, vol. 109, pp. 402–410, 2016.
[23] X. Nie *et al.*, "Carbon quantum dots: A bright future as photosensitizers for in vitro antibacterial photodynamic inactivation," *J Photochem Photobiol B*, vol. 206, p. 111864, 2020.
[24] Z. Zhang *et al.*, "A minireview on doped carbon dots for photocatalytic and electrocatalytic applications," *Nanoscale*, vol. 12, no. 26, pp. 13899–13906, 2020.
[25] C. Zhao *et al.*, "Quaternary ammonium carbon quantum dots as an antimicrobial agent against gram-positive bacteria for the treatment of MRSA-infected pneumonia in mice," *Carbon N Y*, vol. 163, pp. 70–84, 2020.
[26] X. Wei *et al.*, "Facile synthesis of a carbon dots and silver nanoparticles (CDs/AgNPs) composite for antibacterial application," *RSC Adv*, vol. 11, no. 30, pp. 18417–18422, 2021.
[27] X. Nie *et al.*, "Carbon quantum dots: A bright future as photosensitizers for in vitro antibacterial photodynamic inactivation," *J Photochem Photobiol B*, vol. 206, p. 111864, 2020.
[28] Y. Su, B. Shi, S. Liao, J. Zhao, L. Chen, and S. Zhao, "Silver nanoparticles/N-doped carbon-dots nanocomposites derived from siraitia grosvenorii and its logic gate and surface-enhanced raman scattering characteristics," *ACS Sustain Chem Eng*, vol. 4, no. 3, pp. 1728–1735, 2016.
[29] W.-J. Niu, R.-H. Zhu, H.-B. Zeng, S. Cosnier, X.-J. Zhang, and D. Shan, "One-pot synthesis of nitrogen-rich carbon dots decorated graphene oxide as metal-free electrocatalyst for oxygen reduction reaction," *Carbon N Y*, vol. 109, pp. 402–410, 2016.
[30] B. Valdez-Salas *et al.*, "Promotion of surgical masks antimicrobial activity by disinfection and impregnation with disinfectant silver nanoparticles," *Int J Nanomedicine*, pp. 2689–2702, 2021.
[31] C. B. Hiragond, A. S. Kshirsagar, V. V Dhapte, T. Khanna, P. Joshi, and P. V More, "Enhanced anti-microbial response of commercial face mask using colloidal silver nanoparticles," *Vacuum*, vol. 156, pp. 475–482, 2018.
[32] Y. Li, P. Leung, L. Yao, Q. W. Song, and E. Newton, "Antimicrobial effect of surgical masks coated with nanoparticles," *Journal of Hospital Infection*, vol. 62, no. 1, pp. 58–63, 2006.
[33] S. S. Suner, M. Sahiner, R. S. Ayyala, V. R. Bhethanabotla, and N. Sahiner, "Nitrogen-doped arginine carbon dots and its metal nanoparticle composites as antibacterial agent," *C (Basel)*, vol. 6, no. 3, p. 58, 2020.

[34] Z. Ma, Q. Jia, C. Tao, and B. Han, "Highlighting unique function of immobilized superoxide on TiO2 for selective photocatalytic degradation," *Sep Purif Technol*, vol. 238, p. 116402, May 2020, doi: 10.1016/J.SEPPUR.2019.116402.
[35] C.-Y. Hsu, P.-Y. Chao, S.-P. Hu, and C.-M. Yang, "The Antioxidant and Free Radical Scavenging Activities of Chlorophylls and Pheophytins," *Food Nutr Sci*, vol. 04, no. 08, pp. 1–8, 2013, doi: 10.4236/fns.2013.48a001.
[36] H. Ji, F. Zhou, J. Gu, C. Shu, K. Xi, and X. Jia, "Nitrogen-Doped Carbon Dots as A New Substrate for Sensitive Glucose Determination," *Sensors 2016, Vol. 16, Page 630*, vol. 16, no. 5, p. 630, May 2016, doi: 10.3390/S16050630.
[37] X. Zhou *et al.*, "Nitrogen-doped carbon dots with high quantum yield for colorimetric and fluorometric detection of ferric ions and in a fluorescent ink," *Microchimica Acta*, vol. 186, no. 2, pp. 1–9, Feb. 2019, doi: 10.1007/S00604-018-3176-9/FIGURES/2.
[38] H. Wang *et al.*, "Nitrogen-doped carbon dots for 'green' quantum dot solar cells," *Nanoscale Res Lett*, vol. 11, no. 1, pp. 1–6, Jan. 2016, doi: 10.1186/S11671-016-1231-1/FIGURES/5.
[39] X. Wei *et al.*, "Facile synthesis of a carbon dots and silver nanoparticles (CDs/AgNPs) composite for antibacterial application †," 2021, doi: 10.1039/d1ra02600c.
[40] W. W. W. Melkamu and L. T. Bitew, "Green Synthesis of Silver Nanoparticles Using *Hagenia abyssinica (Bruce) J.F. Gmel* Plant Leaf Extract and Its Antibacterial and Anti-Oxidant Activities," *SSRN Electronic Journal*, Aug. 2021, doi: 10.2139/SSRN.3895676.
[41] J. C. Jin *et al.*, "One-step synthesis of silver nanoparticles using carbon dots as reducing and stabilizing agents and their antibacterial mechanisms," *Carbon N Y*, vol. 94, pp. 129–141, Nov. 2015, doi: 10.1016/J.CARBON.2015.05.084.
[42] R. Atchudan, T. N. J. I. Edison, K. R. Aseer, S. Perumal, and Y. R. Lee, "Hydrothermal conversion of Magnolia liliiflora into nitrogen-doped carbon dots as an effective turn-off fluorescence sensing, multi-colour cell imaging and fluorescent ink," *Colloids Surf B Biointerfaces*, vol. 169, pp. 321–328, Sep. 2018, doi: 10.1016/j.colsurfb.2018.05.032.
[43] L. Wang and H. S. Zhou, "Green synthesis of luminescent nitrogen-doped carbon dots from milk and its imaging application," *Anal Chem*, vol. 86, no. 18, pp. 8902–8905, Sep. 2014, doi: 10.1021/ac502646x.
[44] N. Hashemi and M. H. Mousazadeh, "Preparation of fluorescent nitrogen-doped carbon dots for highly selective on-off detection of Fe3+ ions in real samples," *Opt Mater (Amst)*, vol. 121, Nov. 2021, doi: 10.1016/j.optmat.2021.111515.
[45] T. Dutta, N. N. Ghosh, M. Das, R. Adhikary, V. Mandal, and A. P. Chattopadhyay, "Green synthesis of antibacterial and antifungal silver nanoparticles using Citrus limetta peel extract: Experimental and theoretical studies," *J Environ Chem Eng*, vol. 8, no. 4, p. 104019, Aug. 2020, doi: 10.1016/J.JECE.2020.104019.
[46] X. Wei *et al.*, "Facile synthesis of a carbon dots and silver nanoparticles (CDs/AgNPs) composite for antibacterial application," *RSC Adv*, vol. 11, no. 30, pp. 18417–18422, May 2021, doi: 10.1039/D1RA02600C.
[47] L. Salvioni *et al.*, "Negatively charged silver nanoparticles with potent antibacterial activity and reduced toxicity for pharmaceutical preparations," *Int J Nanomedicine*, vol. 12, pp. 2517–2530, Mar. 2017, doi: 10.2147/IJN.S127799.
[48] H. R. Hong, J. Kim, and C. H. Park, "Facile fabrication of multifunctional fabrics: use of copper and silver nanoparticles for antibacterial, superhydrophobic, conductive fabrics," *RSC Adv*, vol. 8, no. 73, pp. 41782–41794, Dec. 2018, doi: 10.1039/C8RA08310J.
[49] U. Siripatrawan and W. Vitchayakitti, "Improving functional properties of chitosan films as active food packaging by incorporating with propolis," *Food Hydrocoll*, vol. 61, pp. 695–702, Dec. 2016, doi: 10.1016/J.FOODHYD.2016.06.001.
[50] S. Kadian, G. Manik, N. Das, P. Nehra, R. P. Chauhan, and P. Roy, "Synthesis, characterization and investigation of synergistic antibacterial activity and cell viability of silver-sulfur doped graphene quantum dot (Ag@S-GQDs) nanocomposites," *J Mater Chem B*, vol. 8, no. 15, pp. 3028–3037, Apr. 2020, doi: 10.1039/c9tb02823d.
[51] H. Kong and J. Jang, "Antibacterial Properties of Novel Poly(methyl methacrylate) Nanofiber Containing Silver Nanoparticles," *Langmuir*, vol. 24, no. 5, pp. 2051–2056, Mar. 2008, doi: 10.1021/la703085e.
[52] H. Qian *et al.*, "Mussel-inspired superhydrophobic surfaces with enhanced corrosion resistance and dual-action antibacterial properties," *Materials Science and Engineering: C*, vol. 80, pp. 566–577, Nov. 2017, doi: 10.1016/J.MSEC.2017.07.002.